

## Purdue University Purdue e-Pubs

---

International Refrigeration and Air Conditioning  
Conference

School of Mechanical Engineering

---

2018

# Numerical Investigation of a Forced-Air Cooled Condenser Using 1d-3d-Coupling

Bernhard Zuber

*Graz University of Technology, Austria, zuber@ivt.tugraz.at*

Johann Hopfgartner

*Institute for Internal Combustion Engines and Thermodynamics, Austria, hopfgartner@ivt.tugraz.at*

Andreas Egger

*Graz University of Technology, Austria, egger@ivt.tugraz.at*

Raimund Almbauer

*Graz University of Technology, Austria, almbauer@ivt.tugraz.at*

Follow this and additional works at: <https://docs.lib.purdue.edu/iracc>

---

Zuber, Bernhard; Hopfgartner, Johann; Egger, Andreas; and Almbauer, Raimund, "Numerical Investigation of a Forced-Air Cooled Condenser Using 1d-3d-Coupling" (2018). *International Refrigeration and Air Conditioning Conference*. Paper 2029.  
<https://docs.lib.purdue.edu/iracc/2029>

This document has been made available through Purdue e-Pubs, a service of the Purdue University Libraries. Please contact [epubs@purdue.edu](mailto:epubs@purdue.edu) for additional information.

Complete proceedings may be acquired in print and on CD-ROM directly from the Ray W. Herrick Laboratories at <https://engineering.purdue.edu/Herrick/Events/orderlit.html>

## Numerical investigation of a forced-air cooled condenser using 1D-3D-coupling

Bernhard ZUBER<sup>1\*</sup>, Johann HOPFGARTNER<sup>1</sup>, Andreas EGGER<sup>1</sup>, Raimund ALMBAUER<sup>1</sup>

<sup>1</sup>Graz University of Technology, Institute of Internal Combustion Engines and Thermodynamics,  
Inffeldgasse 19, 8010 Graz, Austria

zuber@ivt.tugraz.at	+43 316 873 30235
hopfgartner@ivt.tugraz.at	+43 316 873 30240
egger@tugraz.at	+43 316 873 30234
almbauer@tugraz.at	+43 316 873 30230

\* Corresponding Author

### ABSTRACT

To further improve the efficiency of refrigerators and freezers, it is necessary to optimize the whole cooling cycle. With one-dimensional numerical simulation programs, the transient behavior of the refrigeration cycle over more than 24 hours can be calculated. A major challenge here is to find appropriate heat transfer coefficients especially when the heat transfer is mainly influenced by forced-ventilation. In the present paper a wine cooler with a forced-air cooled condenser is investigated. To take the influences of the air flow and the condenser geometry on the simulated heat transfer into consideration, three-dimensional flow simulations are used.

Due to superheating, subcooling and the transient behavior, the temperature varies across the condenser. Since the transferred heat strongly depends on the distribution of the temperature across the condenser surface, it would be necessary to run the 3D-CFD-simulation after every time step of the 1D simulation. To avoid this tremendous numerical effort, a more efficient method with so-called factors of influence is introduced. These factors of influence are calculated, using the results of around 30 CFD simulations, which are performed with different temperature distributions. After the determination of these factors, the heat transfer for a given condenser geometry can be calculated for different temperature distributions with a simple algebraic equation. To validate this procedure, CFD simulations with random temperature distributions are performed and compared with the results of the new method. The developed method has been implemented into the 1D cycle simulation. Thus it is possible to consider the geometry of the condenser and the complex flow field in the 1D simulation without a noticeable increase of the computational effort. Finally the results of the cycle simulation are validated with measurement results.

### 1 INTRODUCTION

In order to counteract the trend of increasing global energy consumption, guidelines for labelling energy efficiency have been introduced in many areas. These easy-to-compare labels and consumers' increased environmental awareness pose major challenges to manufacturers of household refrigerators and freezers. Due to the high and ever increasing number of devices, the share of the total energy consumption is considerable. Studies (IEA, 2009) show that in the EU, about 15% of households electrical energy consumption is used for refrigeration appliances. The average energy consumption of a household refrigeration unit is given as 1kWh/day according to Hermes and Melo (2008). This results in an annual energy consumption of about 22TWh for Germany, see BDEW (2014). In order to reach these efficiency goals and also shorten the development process more and more computer-aided simulation tools are used. In this work an in-house developed transient one-dimensional simulation program is used (Heimel *et al.*, 2015 and Heimel *et al.*, 2016). In this software all relevant components of the refrigeration cycle are modelled. The heat transfer at the condenser surface has a major impact on the whole refrigeration cycle and the energy consumption. To decrease the temperature of the condenser and therefore increase the efficiency more and more manufacturer use forced-air cooled condensers. In this work a wine cooler with a forced-air cooled condenser is investigated. To examine the air flow around the condenser a three-dimensional CFD simulation is used. To integrate the results of the CFD simulation in the 1D cycle simulation a new method is introduced.

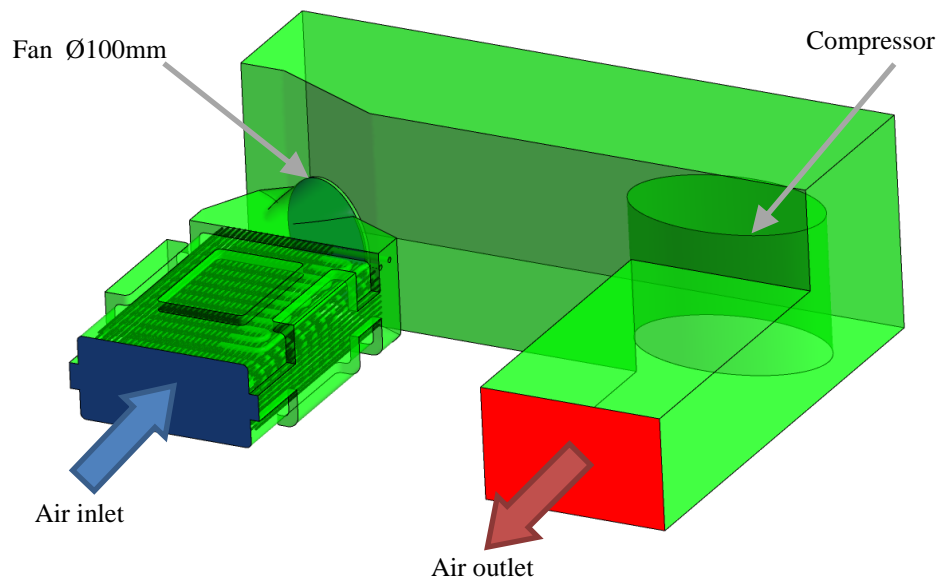
## 2 3D CFD SIMULATION

The main focus of the CFD simulations is the investigation of the heat transfer between the air and the condenser surface. Due to the high number of fins, the geometry of the condenser is very complex. In addition, a relatively fine mesh is needed near the condenser surface to calculate the heat transfer accurately. Therefore, a simulation of the entire condenser for the determination of the heat transfer is not possible with the available computing power. For this reason, only a quarter of the condenser is simulated, which is discussed in chapter 2.2. However, a simulation of the entire base is needed to determine the overall air flow rate. Therefore, a second simulation of the whole base with a much coarser mesh and with deactivated energy equation is performed.

All CFD simulations are carried out as steady-state simulations using a coupled solver. The turbulence is modelled with the RANS approach using the  $k-\omega$ -SST turbulence model. The air is modelled as an incompressible ideal gas using temperature dependent polynomials for viscosity and thermal conductivity.

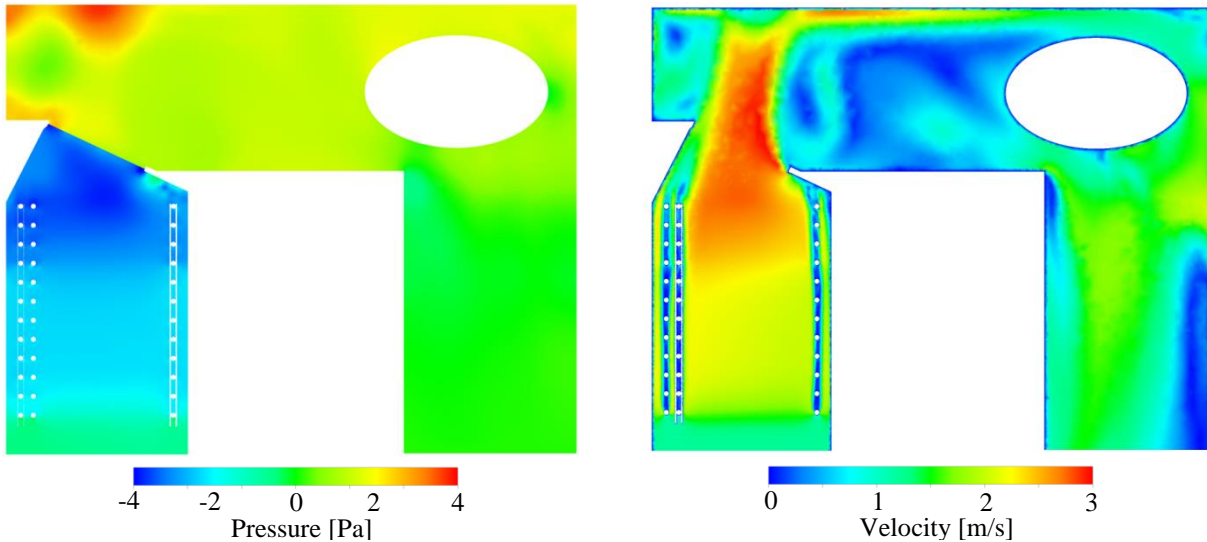
### 2.1 Flow simulation of the entire base

Figure 1 shows the geometry of the base. The air enters at the front of the wine cooler, flows over the condenser surface, through the 100mm-fan, around the compressor and exits again at the front. For the simulation a few simplifications are assumed. The modelling of the moving fan blades is not possible in the steady state flow simulation. Therefore, the fan is modelled as an interface with a volume flow dependent pressure jump. This relation between volume flow and pressure difference is taken from the fan characteristics provided by the manufacturer. Since the fan is located after the condenser the simplification has only a small influence on the flow over the condenser surface. The refrigerant tubes in the back of the base are not modelled and the compressor and the geometry of the housing are replaced with simpler geometries.



**Figure 1:** Geometry of the base

Since only the pressure loss and the resulting flow rate are of interested, the energy equation is deactivated. At the air inlet and air outlet a total pressure boundary condition is set. Figure 2 shows the pressure and velocity distribution in a horizontal cutting plain. The pressure jump at the fan interface is clearly visible. The simulation adjusts the volume flow using the fan characteristic, which results in an air volume flow of around 50m<sup>3</sup>/h. This volume flow is used to carry out the further flow simulations in chapter 2.2. In the velocity distribution it can be seen that the fan is not modelled correctly due to the selected boundary condition. With the actual fan blades, the air would rather flow parallel to the fan axis. Furthermore, the rotation and turbulence introduced by the fan have been neglected.



**Figure 2:** Pressure and Velocity in base

## 2.2 Simulation of flow around condenser

The mesh used to simulate the base is not suitable for calculating the heat transfer at the condenser surface. The number of cells around the condenser and especially at the condenser fins is too low. To determine the heat transfer, the simulation of the entire base is not necessary. Therefore, only the part of the base that is in front of the fan needs to be simulated. To further decrease the computational effort only a quarter of the condenser is simulated. On the left in Figure 3 the geometry of the condenser without fins is shown. On the right in Figure 3 the simulated region is highlighted.

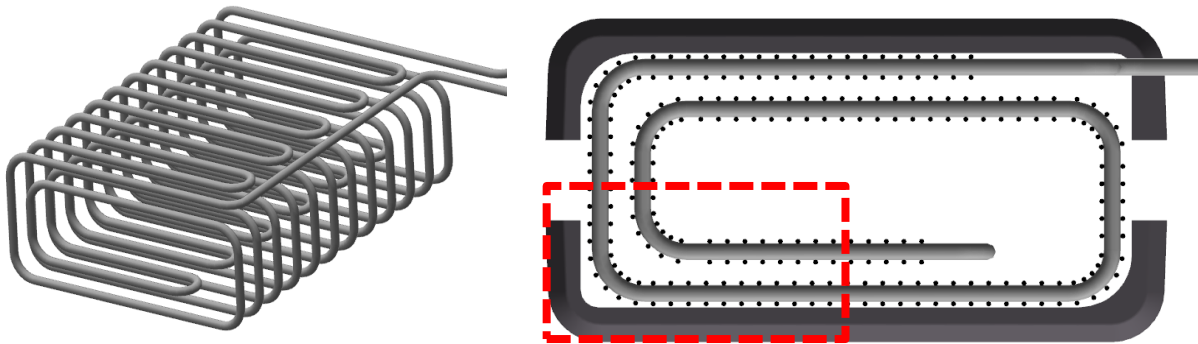


**Figure 3:** Condenser geometry (without fins) and simulated region

In the 1D cycle simulation, the condenser tube is divided into cells. The temperature of these cells is not constant over the entire condenser. Temperature differences can occur due to superheating at the inlet of the condenser, subcooling at the outlet or due to the unsteady operation of the system. To take these different temperatures into account in the flow simulation, it is necessary to divide the condenser surface similarly to the 1D cycle simulation. The surface was split into 24 areas as shown in Figure 4. The condenser is subdivided into twelve tube rows and into an outer and inner tube position. The outer tubes are very close to the housing wall. Therefore, it is to be expected that the heat flux differs from the inner position.

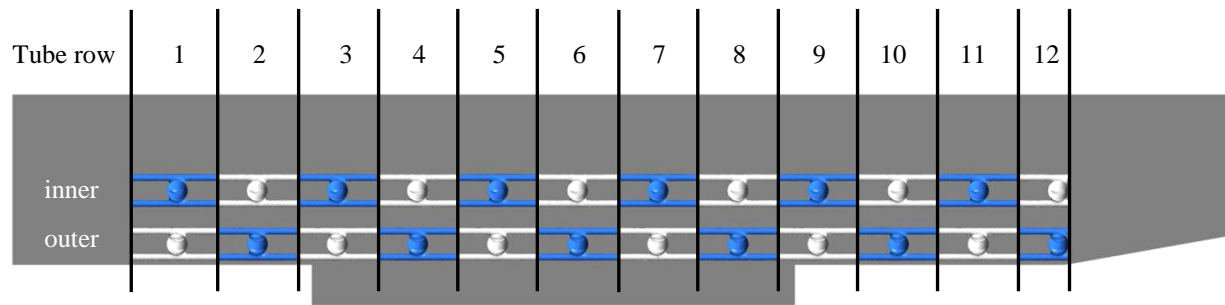


**Figure 4:** Discretization of condenser surface

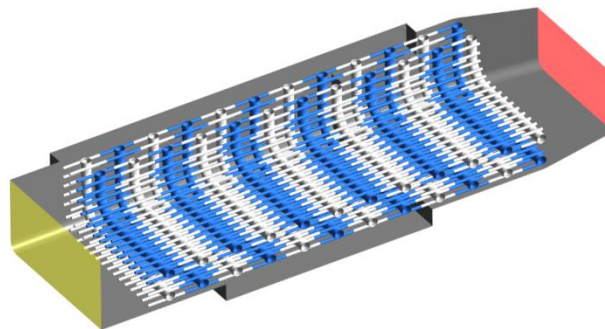


**Figure 5:** Boundary surfaces of mesh

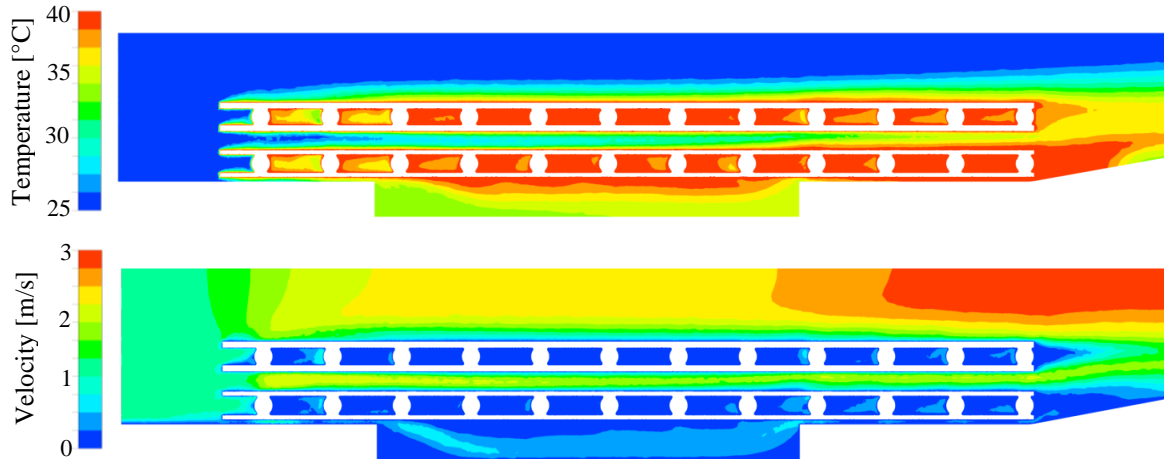
In Figure 5 the boundaries of the mesh are displayed. At the inlet (yellow) a constant velocity boundary condition is set. For the outlet (red) a constant pressure boundary condition is used. At the walls of the channel a wall boundary condition with no heat flux is set. For the 24 condenser surfaces (white and blue) the wall temperatures are set. Since only a quarter of the condenser is simulated the cutting planes are modelled as symmetry planes.

Due to the complex geometry an unstructured mesh of tetrahedral cells is used. A finer resolution of the near-wall regions with prism layers is not possible, since the number of computational cells increases too much even with only a few layers. The computational grid used for the simulation consisted of around 8.1 million cells with a minimal cell length of 0.5mm at the fin surface. In order to verify the independence of the simulation results from the computational grid, simulations with different mesh sizes were performed. Table 1 shows the results of this mesh study. The heat flux changes by about 2% from the mesh with around 4 million cells to the mesh with 8 million cells. With a further refinement to 16 million cells, the heat flux changes only by about 0.2%. Therefore, it can be assumed that the grid with 8 million cells gives sufficiently accurate results.

Table 1: Result of mesh study

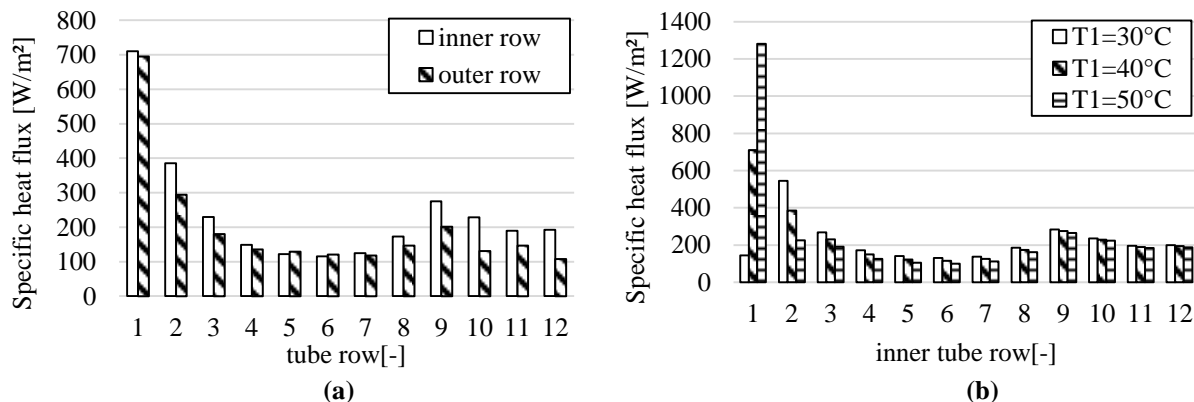
Cell count	Minimal cell length	Specific heat flux, total [W/m <sup>2</sup> ]	Specific heat flux, first row [W/m <sup>2</sup> ]
4,320,445	0.7 mm	226.0 (1.85%)	708.7 (-0.79%)
<b>8,145,369</b>	0.5 mm	221.9	714.4
15,990,679	0.35 mm	221.5 (-0.18%)	713.6 (-0.11%)

Figure 6 shows the temperature and velocity distribution of the air in the direction of flow. It can be seen that the air flowing over the fins almost reaches the surface temperature of 40°C. A large part flows through the centre of the condenser without coming close to the condenser surface and therefore hardly heats up. The velocity distribution shows that the velocity is highest in the middle of the condenser and very low at the condenser tubes close to the wall. Therefore, the heat flow is lower at the outer tube rows near the wall than at the inner tube rows.



**Figure 6:** Temperature and velocity of air flow around condenser

Figure 7a shows the calculated specific heat fluxes at an ambient temperature of 25°C and a constant temperature profile of 40°C over the whole condenser. The specific heat flux is highest at the first row and continues to decrease from row to row. At row eight the heat flow increases again. The reason for this is that there is a step in the condenser housing which leads to a slightly inclined flow and a better mixing of the air. As expected, the heat flow at the inner tube position is slightly higher than at the outer position close to the wall.



**Figure 7:** Specific heat flux at (a) 40°C surface temperature, (b) temperature of first row varied

For the sake of clarity, only the heat fluxes of the inner tube position are shown in Figure 7b. In addition to the result of the simulation with constant temperature profile, two cases in which the temperature of the first row is increased and decreased by 10K are shown. By changing the temperature, the transferred heat changes at the first row, but also the other rows are affected. If more heat is transferred at the first row of tubes, the air temperature at the other rows is already higher and thus the transferred heat lower. Therefore, the transferred heat depends on the temperature distribution at the condenser. Thus, it is necessary to transfer these results into the model of the 1D cycle simulation. Therefore a new method was developed, which will be described in chapter 4.

### 3 1D CYCLE SIMULATION

The basis for this work is a transient one-dimensional cycle simulation program developed in house by Heimele et al. (2015, 2016). This program allows the numerical simulation of the entire device. Since the majority of the currently used devices are controlled by switching the compressor on and off, the cyclic transient behaviour must be simulated. Therefore, it is necessary to perform the cycle simulation transiently. With this simulation program, it is possible to calculate the cyclical operation of refrigerators for a period of several hours. The simulation is resolved in time with a time step of about one second. The calculation of the simulation requires approximately one fifth of the simulated time. This makes it possible to calculate a 24-hour cycle in a reasonable time. In the simulation

software all relevant components are modelled. The capillary model was developed by Heimel et al. (2014) using an artificial neural network approach. The compressor model was validated with transient measurements (Posch et al. 2014) (Li 2012). The condenser and evaporator model are modelled with a finite volume approach. The model of the condenser is described in more detail in the next sub chapter.

### 3.1 1D-Modelling of condenser

The condenser is subdivided into a finite number of elements using the finite-volume method. For the refrigerant, the continuity equation and the energy equation are solved in every volume. In the condenser, a phase transition takes place, from the gaseous refrigerant at the inlet to liquid refrigerant at the outlet. In between lays the two-phase region in which both phases occur side by side. It is assumed that the two phases are in thermal equilibrium. Flow regime based correlations for pressure drop (QuiBen and Thome, 2007), heat transfer (Thome *et al.*, 2003) and void fraction (El Hajal *et al.*, 2003) are implemented. The model is able to consider slip between gaseous and liquid phase. The steel-tube including its thermal inertia is also implemented and strongly influences the dynamic behavior of the condensing pressure. Also the heat transfer along the condenser tube and along the fins is implemented. For more information, the work of Berger *et al.* (2015) is recommended.

For the heat transfer at the condenser surface only a simple model for free convection was implemented. Since forced convection occurs in this case, this model is not applicable. The heat transfer at the forced-ventilated condenser depends very much on the geometry and the air flow. For a more detailed modelling of the heat transfer, the results of the 3D CFD simulation have to be implemented into the cycle simulation.

## 4 1D-3D COUPLING

The goal of the coupling is to determine the distribution of the heat flux for a given condenser temperature profile in the cycle simulation. Since a CFD simulation for every temperature profile is much too time consuming, it is necessary to find a more efficient method. At first the use of look up tables was investigated. The flow simulation is carried out for different temperature profiles and the results are stored. From these tables, the heat fluxes can now be calculated by interpolation for any temperature profile. To cover all cases, many combinations of the individual temperatures must be calculated. The number of simulations required is calculated from the number of rows and the number of temperature support points.

$$N_{sim} = N_{temp}^{N_{rows}} \quad (1)$$

However, this method is not suitable for the condenser with twelve rows. With only three temperature points it would take more than half a million simulations to cover all combinations.

### 4.1 Method of influence factors

To reduce the computational effort, it is necessary to develop a method that works with as few CFD simulations as possible. The aim of this method is to reproduce the CFD results as accurately as possible, without increasing the computational effort of the 1D cycle simulation.

As the basis of this method, the heat transfer at constant temperature over the entire condenser was calculated. These cases are referred to as isothermal (iso). To determine the temperature dependency, simulations were performed at several condenser temperatures. The specific heat flow for the isothermal case  $q_{iso_i}(T)$  can be linearly interpolated with the simulation results (equation 2). This interpolation is sufficiently accurate even with a few temperature points. For the temperature points, a interval of 10K was chosen. Thus, only about six CFD simulations are needed to cover the relevant temperature range.

$$q_{iso_i}(T) = q_{iso_i}(T_{sim_l}) + \frac{q_{iso_i}(T_{sim_u}) - q_{iso_i}(T_{sim_l})}{T_{sim_u} - T_{sim_l}} T \quad (2)$$

In order to describe the influence of the deviation of a temperature from the isothermal case, so-called influencing factors  $f_{ij}$  were introduced. The definition of these factors is the ratio of the change in the heat flux at the i-th tube to the change in the heat flux at the j-th tube. As reference the results of the isothermal cases are used.

$$f_{ij} = \frac{\Delta q_i}{\Delta q_j} = \frac{q_i - q_{iso,i}(T_i)}{q_j - q_{iso,j}(T_i)} \quad (3)$$

If these influencing factors are known, the specific heat flux can be calculated according to the following equation:

$$q_i = q_{iso,i}(T_i) - \sum_j^{j=n_{tubes}} f_{ij} \cdot (q_j - q_{iso,j}(T_i)) \quad \text{with } f_{ii} = 0 \quad (4)$$

Starting from the isothermal heat flux  $q_{iso,i}(T_i)$ , the actual heat flow  $q_i$  is calculated. The factor  $f_{ii}$  is zero, since an influence factor of the pipe on itself makes no sense. To calculate the heat flux at the  $i$ -th tube, the heat fluxes on all other tubes must be known. In order to solve this equation it has to be transformed.

$$1 \cdot q_i + \sum_j^{j=n_{tubes}} f_{ij} q_j = 1 \cdot q_{iso,i}(T_i) + \sum_j^{j=n_{tubes}} f_{ij} \cdot q_{iso,j}(T_i) \quad (5)$$

$$\sum_j^{j=n_{tubes}} f'_{ij} q_j = \sum_j^{j=n_{tubes}} f'_{ij} \cdot q_{iso,j}(T_i) \quad (6)$$

The factors  $f'_{ij}$  are equal to  $f_{ij}$  except  $f'_{ii} = 1$ . The reason for this is that the term  $1 \cdot q_i$  is added to the sum. This formula can also be written in matrix notation. Where the operator  $\otimes$  stands for an element-wise multiplication of two matrices and  $\vec{1}$  is a vector, in which each entry has the value 1.

$$\vec{f}' \cdot \vec{q} = (\vec{f}' \otimes \vec{q}_{iso}) \cdot \vec{1} \quad (7)$$

This equation can be solved by multiplication with the inverse of the matrix of influencing factors for  $\vec{q}$ . Thus, the heat flows can be calculated directly from the temperatures and the influencing factors.

$$\vec{q} = \vec{f}'^{-1} \cdot ((\vec{f}' \otimes \vec{q}_{iso}) \cdot \vec{1}) \quad (8)$$

The matrix of influencing factors has the dimension 24x24 and thus has 576 entries. After deduction of the 24 factors  $f_{ii}$ , 552 factors have to be determined. In order to determine the interactions of the pipe rows with each other, 24 CFD simulations were carried. In which the temperature of one of the 24 tubes is increased by 5K. From these results the influencing factors can't be determined directly. It was therefore necessary to develop an iterative solver that adapts the influencing factors so that the calculated heat fluxes match those of the 24 simulations as closely as possible. For this purpose, equation 4 was reshaped so that the error of the calculated heat fluxes compared to the CFD results is calculated:

$$err_{i,n_{sim}} = q_{i,n_{sim}} - q_{iso,i}(T_{i,n_{sim}}) - \left( \sum_j^{j=N_{tubes}} f_{ij} \cdot (q_{j,n_{sim}} - q_{iso,j}(T_{i,n_{sim}})) \right) \quad (9)$$

These errors are summed up to a total error across all tubes and simulations. The exponent  $\gamma$  is introduced to increase the weight of larger errors over smaller ones. With an exponent between 2 and 4, the best results could be achieved. The influencing factors are adjusted iteratively until the error reaches a minimum.

$$err = \sum_{n_{sim}}^{n_{sim}=N_{sim}} \left( \sum_i^{i=N_{tubes}} |err_{i,n_{sim}}|^\gamma \right) \quad (10)$$

With this method the influencing factors can be determined from a few CFD simulations. In addition to the 24 simulations with one altered temperature, approximately six simulations with isothermal profile are necessary. Thus, only a total of 30 CFD simulations are necessary. Also, the CFD simulations do not have to be reinitialized each time, but can be started with the result of the previous simulation. This reduces the number of iteration steps required as the flow field changes only slightly. Thus, the computational effort of this method is manageable and the simulation can be performed with a relatively fine mesh.



#### 4.2 Validation of new method

To verify the introduced calculation method, several CFD simulations with different temperature distributions are performed and the results compared to the calculated heat fluxes. In Figure 8 the temperatures were randomly varied between 40 and 45°C. For reasons of clarity, only the results of the inner tube position are shown. The results of the outer row position are similar. The results of the method match the CFD simulation very well with a mean error of 0.1%. In order to test the behaviour of the method with strongly fluctuating temperature profiles in Figure 9 the temperatures of the rows are alternately set to 35 °C and 60 °C. In this case, some rows even have negative heat flux (heat flux from the air to the condenser). Although the temperature differences are very high and the method was validated with completely different temperature profiles the mean error is only about 1%. In conclusion, it can be said that the developed method predicts the results of the CFD-simulation very accurately. Therefore, the method can be integrated into the cycle simulation.

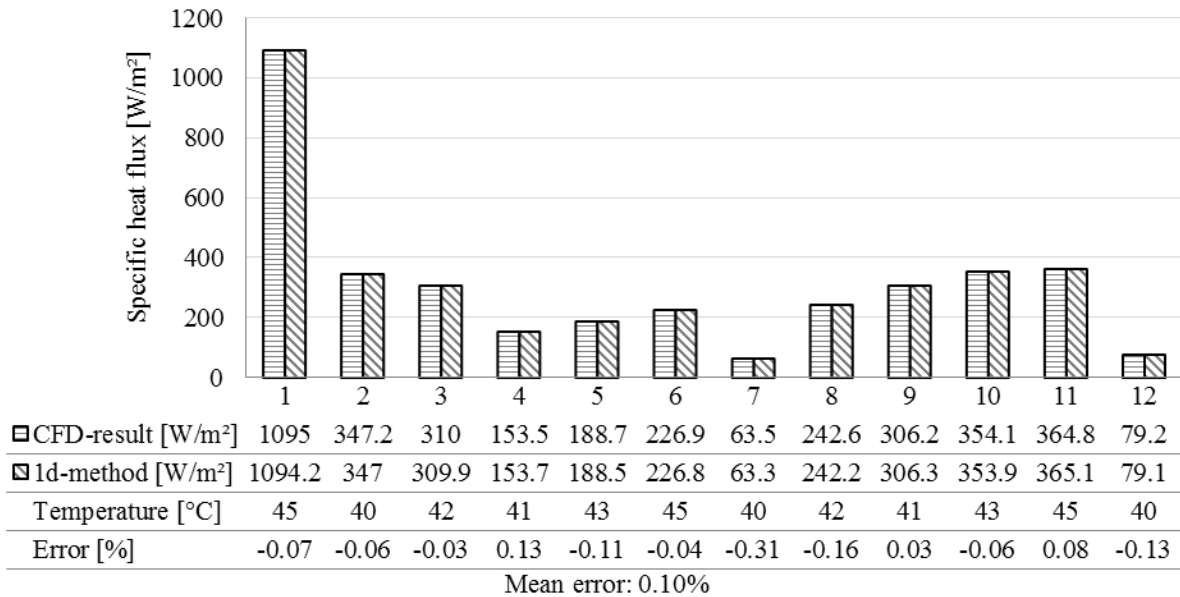


**Figure 8:** Validation with random temperature profile (40-45°C)

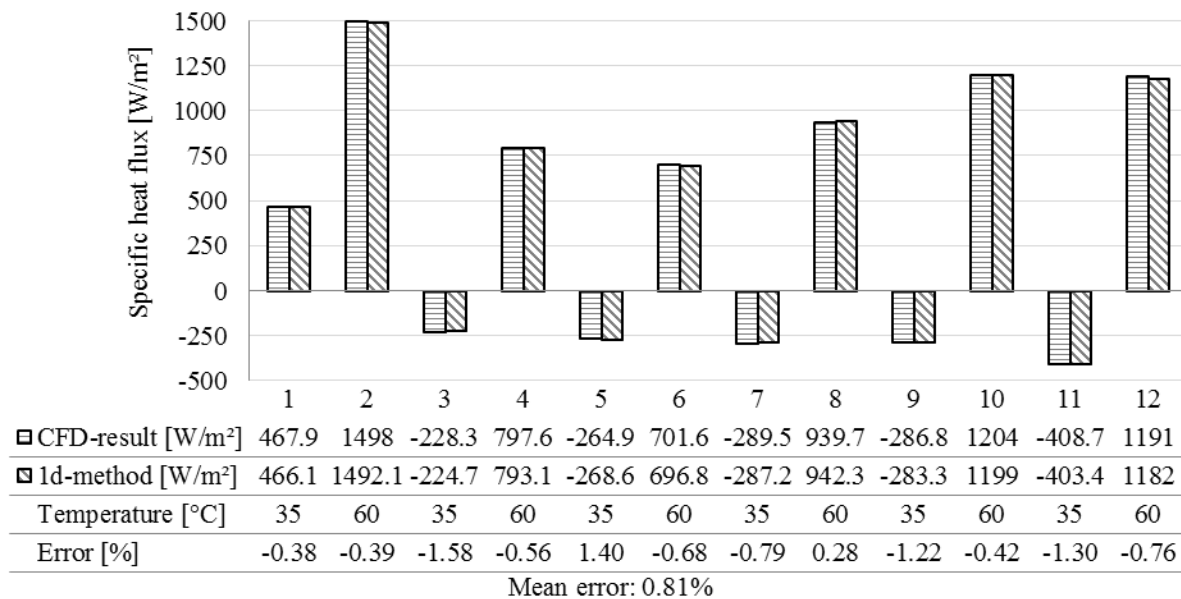


**Figure 9:** Validation with alternating temperatures (35 and 60°C)

## 5 RESULT 1D SIMULATION

The 1D cycle simulation was performed with the coupling method from the previous chapter. For the calibration of the simulation, a standard energy consumption measurement was used. The ambient temperature was 25°C and the compartment temperature was set to 12°C.

To investigate the influence of the air flow rate over the condenser on the overall energy consumption CFD simulations with different flow rates were carried out. When increasing the heat flow, the temperature of the condenser and thus also the condensation pressure of the refrigerant decreases. The increased air flow also increases the electrical power needed by the fan. Figure 10 shows the annual energy consumption of the wine cooler with variation of the air flow rate. In the annual consumption, the increased consumption of the fan is taken into account. The negative influence of the increased fan power is less than the advantage of the lower condenser temperature. Therefore, the annual energy consumption decreases continuously with an increase of the air flow. In reality, there are other limits to the maximum possible air volume flow. These include above all the increasing noise with increasing air speed.

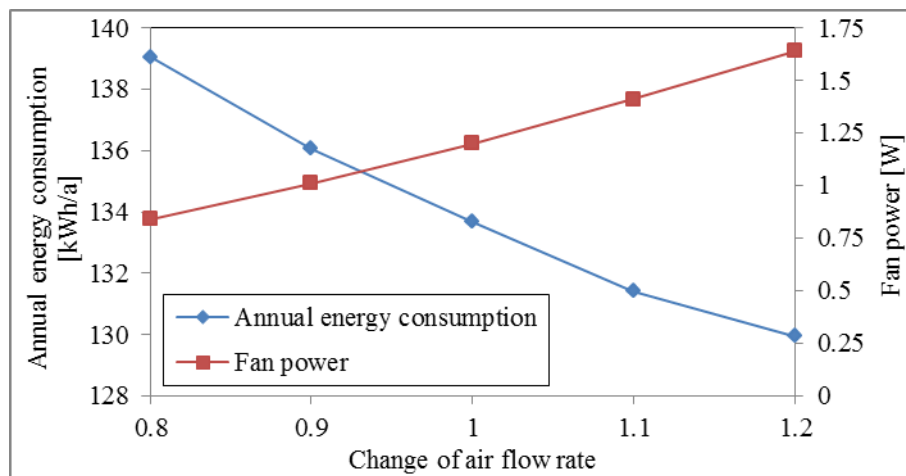


Figure 10: Annual energy consumption and fan power over air flow rate

## 6 CONCLUSION

In this work a wine cooler with a forced-air cooled condenser was investigated using a 1D cycle simulation and 3D CFD simulations. The air flow through the base of the device and especially around the condenser was studied. To take subcooling, superheating and the transient behaviour into account, the condenser surface is split into 24 zones with different surface temperatures. In the CFD simulation the heat fluxes at these zones are calculated. Since this heat fluxes influence each other the CFD simulation has to be carried out for every temperature profile.

To use the CFD results without running a simulation for every temperature profile a new method was developed. In this method so-called influence factors are calculated which describe the influence of the heat fluxes on one another. These factors were determined using the results of about 30 CFD simulations. In these simulations different temperature profiles at the condenser were set. The method was validated with CFD simulations with random temperature profiles.

With this new method it is possible to use the results of the 3D simulation in the 1D cycle simulation without a noticeable increase in computational time. To show the application possibilities the air flow rate in the CFD simulation is varied and the impact on the annual energy consumption is calculated using the cycle simulation.

## REFERENCES

- BDEW (Bundesverband der Energie- und Wasserwirtschaft e.V.) (2014). *Stromverbrauch im Haushalt*. Berlin, Germany.
- Berger, E., Posch, S., HeimeL, M., Almbauer, R., Martin E., & Stupnik, A. (2015). Transient 1D heat exchanger model for the simulation of domestic cooling cycles working with R600a. *Science and Technology for the Built Environment*, 21(7), 1010-1017.
- El Hajal, J., Thome, J. R., & Cavallini, A. (2003). Condensation in horizontal tubes, part 1: two-phase flow pattern map. *Int. J. Heat Mass Tran.*, 46, 3349-3363.
- HeimeL, M., Posch, S., Hopfgartner, J., Berger, E., Stupnik, A., & Almbauer, R. (2015). Simulationsgestützte Optimierung eines Haushaltgefrierschranks. *DKV-Tagung, Dresden, Germany*, AA III.08.
- HeimeL, M., Berger, E., Posch, S., Stupnik, A., Hopfgartner, J., & Almbauer, R. (2016). Transient cycle simulation of domestic appliances and experimental validation. *Int. J. Refrig.*, 69, 28-41.
- HeimeL, M., Lang, W., & Almbauer, R. (2014). Performance predictions using Artificial Neural Network for isobutane flow in non-adiabatic capillary tubes. *Int. J. Refrig.*, 38, 281-289.
- Hermes, C. J., & Melo, C. (2008). A first-principles simulation model for the start-up and cycling transients of household refrigerators, *Int. J. Refrig.*, 31, 1341-1357.
- IEA (International Energy Agency) (2009). *Gadgets and Gigawatts – Policies for Energy Efficient Electronics*. Paris, France: OECD-IEA Publishing.
- Li, W. (2012). Simplified steady-state modelling for hermetic compressors with focus on extrapolation, *Int. J. Refrig.*, 35, 1722-1733.
- Posch, S., Berger, E., HeimeL, M., Almbauer, R., Stupnik, A., & Schoegler H. P. (2014). Comparison and Validation of Semi-empirical Compressor Models for Cycle Simulation Application, *Proc. Int. Compr. Eng. Conf. at Purdue*, Purdue, USA, 1215.
- Quiben, J. M. & Thome, J. R. (2007). Flow pattern based two-phase frictional pressure drop model for horizontal tubes, Part II: New phenomenological model. *Int. J. Heat Fluid Fl.*, 28(5), 1060-1072.
- Thome, J. R., El Hajal, J., & Cavallini, A. (2003). Condensation in horizontal tubes, part 2: new heat transfer model based on flow regimes, *Int. J. Heat Mass Tran.*, 46, 3365-3387.

## NOMENCLATURE

$err$	Error	(-)
$f$	influencing factors	(-)
$N$	amount	(-)
$q$	specific heat flux	(W/m <sup>2</sup> )
$T$	temperature	(°C)
$\gamma$	Exponent	(-)

### Subscripts

i	index
iso	isothermal
j	index
l	lower
n	index
sim	simulations
temp	temperatures
u	upper

## ACKNOWLEDGEMENT

This work was part of ECO-COOL, a research program financed by FFG (Austrian Research Promotion Agency), SFG (Styrian Economic Development), KWF (Kärntner Wirtschaftsförderungsfonds), Standortagentur Tirol and industrial partners.